CZOCHRALSKI RUBY

Annual Technical Summary Report

Period: January 1, 1966 - December 31, 1966

March 20, 1967

Contract No. Nonr-4132(00)

UNION CARBIDE CORPORATION
ELECTRONICS DIVISION

P. O. Box 24184
Indianapolis, Indiana 46224

SRCR-67-5

Contract Nonr-4132(00)
Program Code Number 3730
Authorization ARPA Order 306-62
Task Number NR017-710

CZOCHRALSKI RUBY

Annual Technical Summary Report

Period: January 1, 1966 - December 31, 1966

March 20, 1967

Principal Investigator:
F. R. Charvat

Work Performed and Report Written by:
G. A. Keig
O. H. Nestor
P. E. Otten
J. C. Smith

This research is a part of Project DEFENDER under the joint sponsorship of the Advanced Research Projects Agency, the Office of Naval Research and the Department of Defense.

Union Carbide Corporation
Electronics Division
Crystal Products R and D
P. O. Box 24184
Indianapolis, Indiana 46224

TABLE OF CONTENTS

LIST OF FIGURES

I. INTRODUCTION

The object of this program has been to develop the Czochralski growth technique to yield large ruby crystals with optical quality suitable for use as solid state lasers.

The effort during this past period has been divided into two parts. The first part has been devoted towards a study of the material properties of the ruby with special reference to its behavior during active lasing. This aspect of the work is important as it gives a clearer understanding of the problems involved and allows a more definite effort to be made towards their solution through effective changes in the growth conditions.

The second part describes our efforts in scaling up the present growth process to produce large ruby crystals.

II. RESULTS

A. Material Properties of Ruby Laser Crystals

As part of a continuing program to improve the quality and performance of our ruby laser crystals, two main problems are currently receiving attention. These are: (1) chromium distribution in the crystalline alumina lattice and the inhomogeneities in optical quality associated with localized changes in composition, and (2) the identification and removal of particulate inclusions which are a limiting factor in the power obtainable from a Q-switched laser system. Current research effort in both these areas is described below.

(1) Chromium Distribution

(a) Average Compositional Variations

In this area we have confined our attention to variations in the chrome content along the length of the crystal as well as across the radius. Both of these factors depend on keeping the effective distribution coefficient as close to unity as possible throughout the complete growth cycle; this in turn is a function of interface shape and growth conditions.

In the past we have had considerable success in maintaining a coefficient close to unity; however, further experimentation has shown the sampling procedure used to be somewhat misleading and a systematic variation does occur in the larger diameter ruby boules. Figure 1 shows the percentage variation in chromium content as a function of crystal length for a number of ruby samples. This variation had gone undetected due to the practice of sampling as-grown crystals at the top and bottom only; as indicated in the previous report, these two values were identical and thus it had been assumed that no longitudinal variation existed. This variation must be due to changes in the thermal conditions during crystal growth as it is directly related to the power input from the RF generator.

To maintain the crystal diameter, a balance is required between the heat flow to the growth interface plus the latent heat of solidification, and the heat

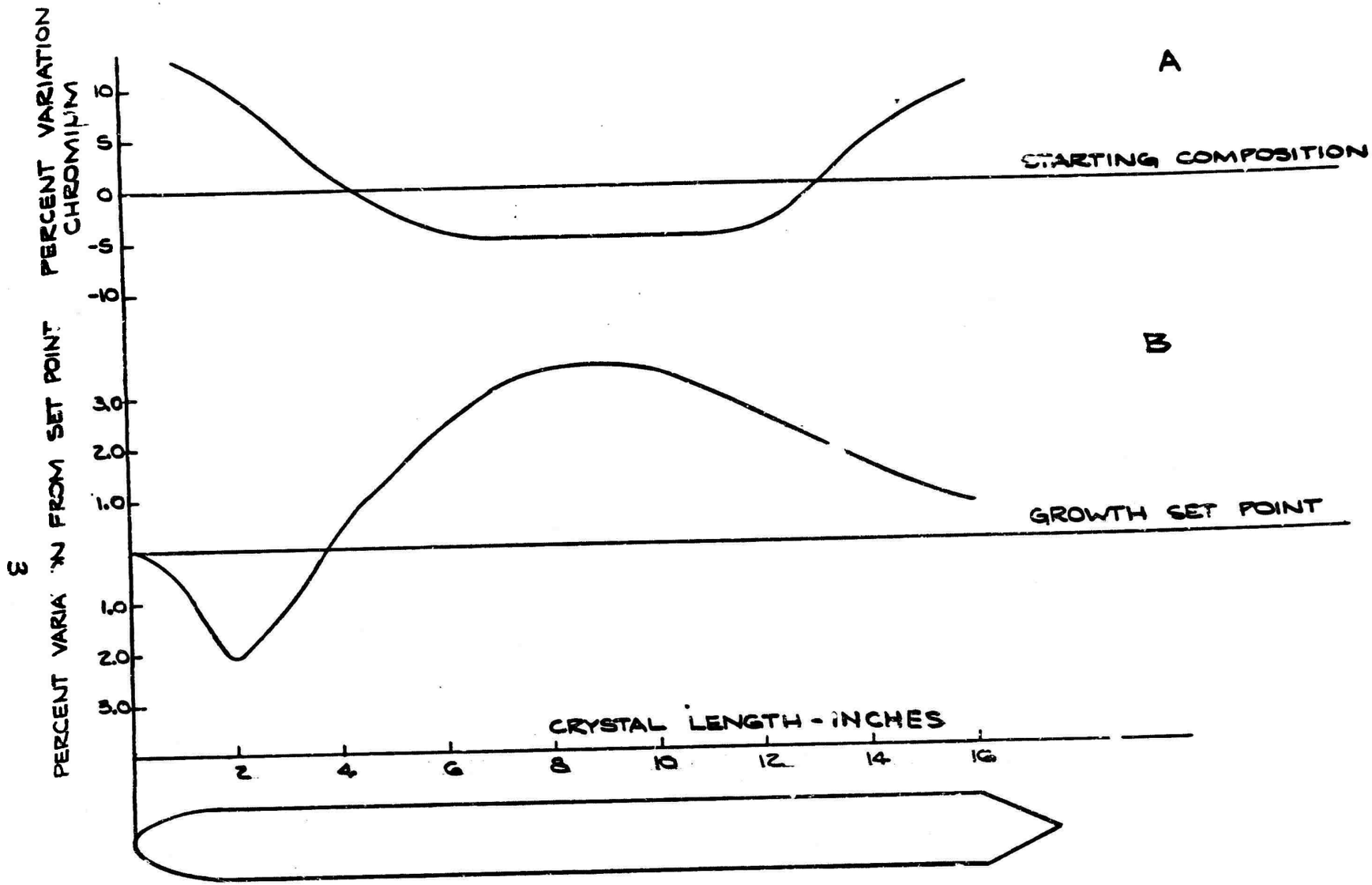

FIG. 1 (A) CHROMIUM CONCENTRATION AND (B) GENERATOR POWER PLOTTED AS A FUNCTION OF CRYSTAL LENGTH

removed by radiation through the solid. At the early stages of growth when the top of the crystal emerges from the furnace insulation, a continuous increase in power to the melt is required. At a critical length, which is a function of crucible and insulation g ometry and crystal diameter, the power requirements level off and are subsequently reduced; this point occurs when a substantial amount of the melt has been used up and the rate of heat removal through the crystal is influenced by the absorption of radiant energy from the hot crucible walls.

An explanation for the observed relationship between the heat flow variations and chromium content in the solid has not been established. However, it is known that the effective distribution coefficient can be changed through variations in both the growth rate and thickness of the diffusion layer along the interface; both of these parameters are influenced by thermal conditions during growth.

Radial chromium variations exist to varying degrees depending on where along the length of the crystal the measurement is made. At the top and bottom where the effective distribution coefficient is significantly greater than one the center portion of the crystal has a lower chromium content than the edge. In the middle of the crystal where the effective distribution coefficient is very clo e to one, the radial chromium gradient is extremely low.

The above observations stress most clearly the need for an effective distribution coefficient of unity throughout the entire growth cycle to eliminate both longitudinal and radial chrome variations. This could best be achieved through manipulation of the appropriate growth parameters, and future experimental work will be carried out along these lines.

(b) Localized Compositional Variations

The core represents an inhomogeneous structure extending throughout the length of the crystal which is associated with the formation of a facet on the interface.[1] This effect is not unique to ruby and is encountered in almost

(1) F. R. Charvat, J. C. Smith, and O. H. Nestor, Characteristics of Large Ruby Crystals, Proceedings of an International Conference on Crystal Growth, Boston, U. S. A., ed. H. S. Peiser, 45-50, June 1966.

all melt-grown crystals, notable examples being doped Ge and Si[2][3], and Nd^{3+} doped YAG.

There is no clearly defined reason for this phenomenon, but generally it can be said that a stable nucleus forms at the interface with an effective distribution coefficient which differs from the average value across the remainder of the interface. The orientation of this stable nucleus is normally a low angle crystallographic plane which in the case of ruby is $\{10\bar{1}1\}$ or $\{0001\}$.

There is a very definite relationship between both the size and distribution of the core and the growth orientation of the crystal. A series of experiments have been carried out with crystals containing a nominal 0.05 wt % Cr_2O_3 grown under identical conditions and using different seed orientation. The facets on the interface were examined closely and their size and shape related to schlieren photographs taken of polished windows cut from the top and bottom of the boule. The boules themselves were also examined and will subsequently be fabricated into laser rods to examine the effect of the core on active lasing.

Examination of crystals grown using seeds of 60° orientation showed that the facets on the interface were positioned corresponding to the "r" planes closest to the growth direction. One "r" plane normal approximately 27° away from the boule axis gave a facet at the tip, whereas as the other normal at approximately 67° to the growth interface produced two relatively large facets; one of these was close to the tip with the other midway along the interface. A schlieren photograph of a polished section of the boule adjacent to the interface showed three distinct cores corresponding to the facets. The core for the facet with normal closest to the growth direction was the most distinct; this core could be seen running through the length of the boule section after flats had been polished on its side. Both the

---

(2) J.A.M. Dikhoff, Cross-sectional Resistivity Variations in Germanium Single Crystals, Solid State Electronics 1, 202-210 (1960).

(3) J.A.M. Dikhoff, Inhomogeneities in Doped Germanium and Silicon Crystals, Philips Technical Review, 25, No. 8, 195-206, 1963/64.

facets on the interface and corresponding schlieren photographs of the adjacent boule sample are shown in Figure 2. Cores corresponding to the facets lying almost tangential to growth interface were not so clearly defined and were unable to be detected from a schlieren taken along the boule length.

A white sapphire boule was grown with the same orientation, and identical facets were observed on the interface. A schlieren photograph of the adjacent boule section showed only a faint core corresponding to the low angle facet at the tip.

The schlieren technique allows a measure to be made of any change in refractive index across a localized region in the crystal. The index variations can arise from a number of different sources, the most important being solute concentration, misorientations, residual stress, and temperature changes[4]. The core in ruby is more pronounced than in white sapphire for crystals grown with identical seed orientation; this indicates clearly the importance of changes in chromium concentration. With white sapphire it is possible that the refractive index changes are caused by residual impurities having a different effective distribution coefficient across the facet. This is consistent with work carried out on undoped InSb[5] where a core was visible with an impurity concentration of approximately 10^{14} atoms/cm^3.

To investigate further the core structure, four ruby boules were grown and are shown in Figure 3. The shape control was good with the average diameter constant down the length of the boule; slight rippling did occur which was attributable to incorrect controller settings. Inspection ends with a six micron diamond finish were fabricated on to the boules and schlieren photographs taken to reveal the shape and size of the core.

---

(4) O. H. Nestor, Refractive Index Variations of Ruby; Beam Divergence and Interferometry, Speedway Research Laboratory Miscellaneous Note No. 37, June 1964.

(5) J. B. Mullin and K. F. Hulme, Orientation-Dependent Distribution Coefficients in Melt Grown InSb Crystals, J. Phys. Chem. Solids, 17, Nos. 1/2, 1-6 (1960).

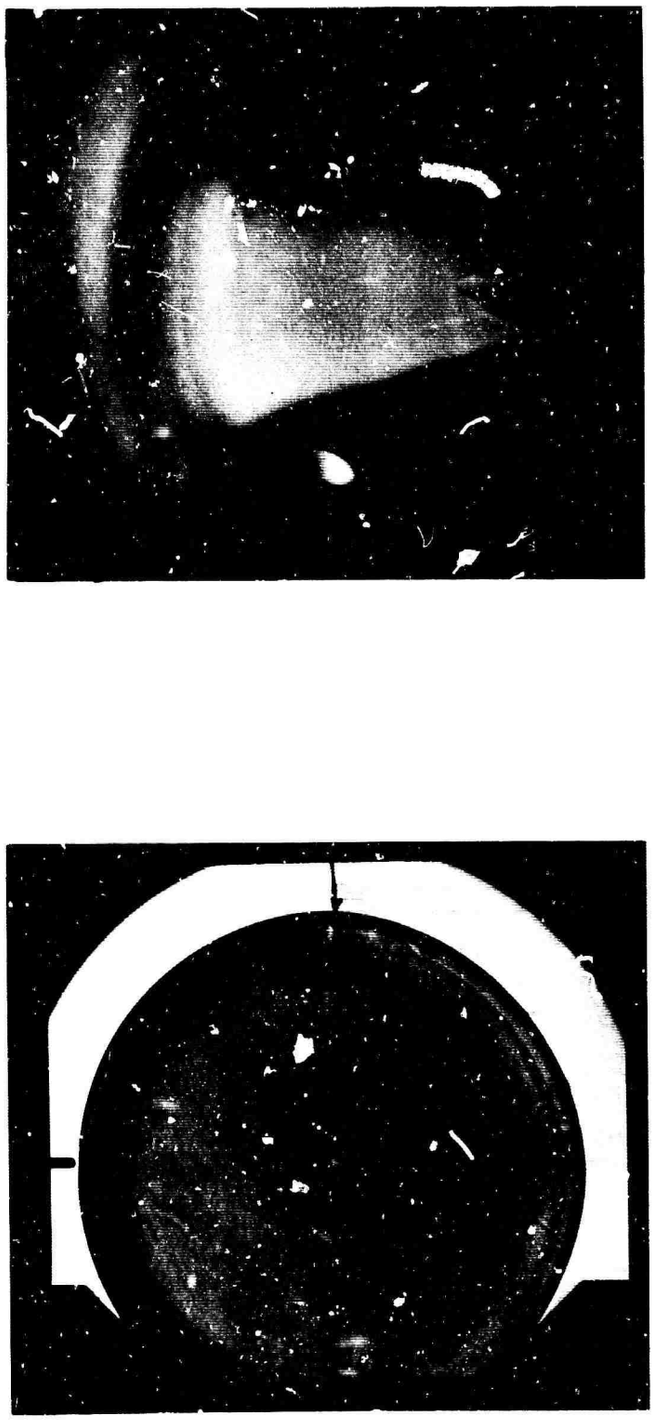

Figure 2. Showing correlation between the facet on the growth interface and the corresponding schlieren photograph.

Figure 3. "As grown" ruby boules with inspection ends.

A set of photographs were taken with the normal orientation technique of lining up the light beam normal to the polished end. These are shown in Figure 4, 6 and 8 for $\vec{E}$ parallel and normal to the plane containing the C axis (in all photographs this plane is vertical). (Results are given for three boules only as the fourth gave no additional information.)

The same rods were then rotated about both the horizontal and vertical position in order to minimize the area of the core; the corresponding schlieren photographs are reproduced in Figures 5, 7, and 9 with $\vec{E}$ parallel to the plane containing the C axis in all cases. Figure 10 indicates the variation in core size and shape which can be obtained with small deliberate changes in the orientation along the horizontal and vertical direction away from that shown in Figure 9. The identification number and orientation of the boules are given in Table I.

TABLE I

Crystal No.	Seed No.	r_1	r_2	r_3	c	a
2500-12-6	103	7			57	46
2500-37-18	152	37-1/2	64	64	60-1/2	32-1/2
2500-10-5	102	27	65-1/2	75	61-1/2	27-1/2
2500-33-16	102	27	65-1/2	75	61-1/2	27-1/2

The above findings point to some important conclusions concerning the core in ruby. With the same seed and under identical growth conditions, it is possible to change the apparent shape and size of the core through slight misorientations in the polished boule face relative to the original growth direction. Consideration of a boule grown from a seed of sixty degree orientatio shows the central core to be about 0.3 mm diameter after corrected alignment; this core corresponds to faceting on the "r" plane with normal 27° to the growth direction.

Previous schlieren photographs taken of a sample with flats polished on the side indicate that this core remains straight and of constant diameter down the length of the boule. The result is to be expected because of the low angle

$\vec{E}$ parallel to C.

$\vec{E}$ perpendicular to C.

Figure 4. Boule No. 2500-12-6 - schlieren taken with light beam normal to inspection face.

Figure 5. Boule No. 2500-12-6 - orientation chosen to eliminate core area.

Figure 6. Boule No. 2500-33-16 - schlieren taken with light beam normal to inspection face.

Figure 7. Boule No. 2500-33-16 - orientation chosen to minimize core area.

$\vec{E}$ parallel to C.

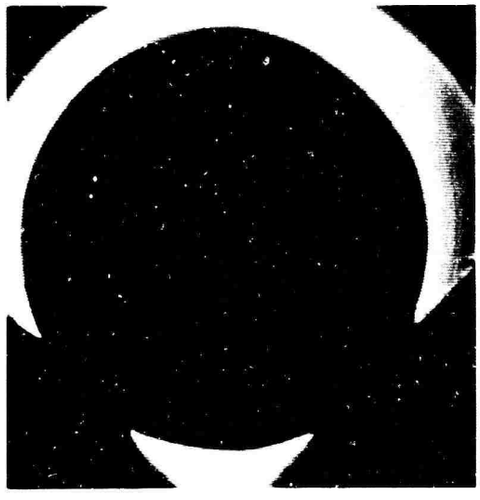

$\vec{E}$ perpendicular to C.

Figure 8. Boule No. 2500-10-5 - schlieren taken with light beam normal to inspection face.

Figure 9. Boule No. 2500-10-5 - orientation chosen to minimize core area.

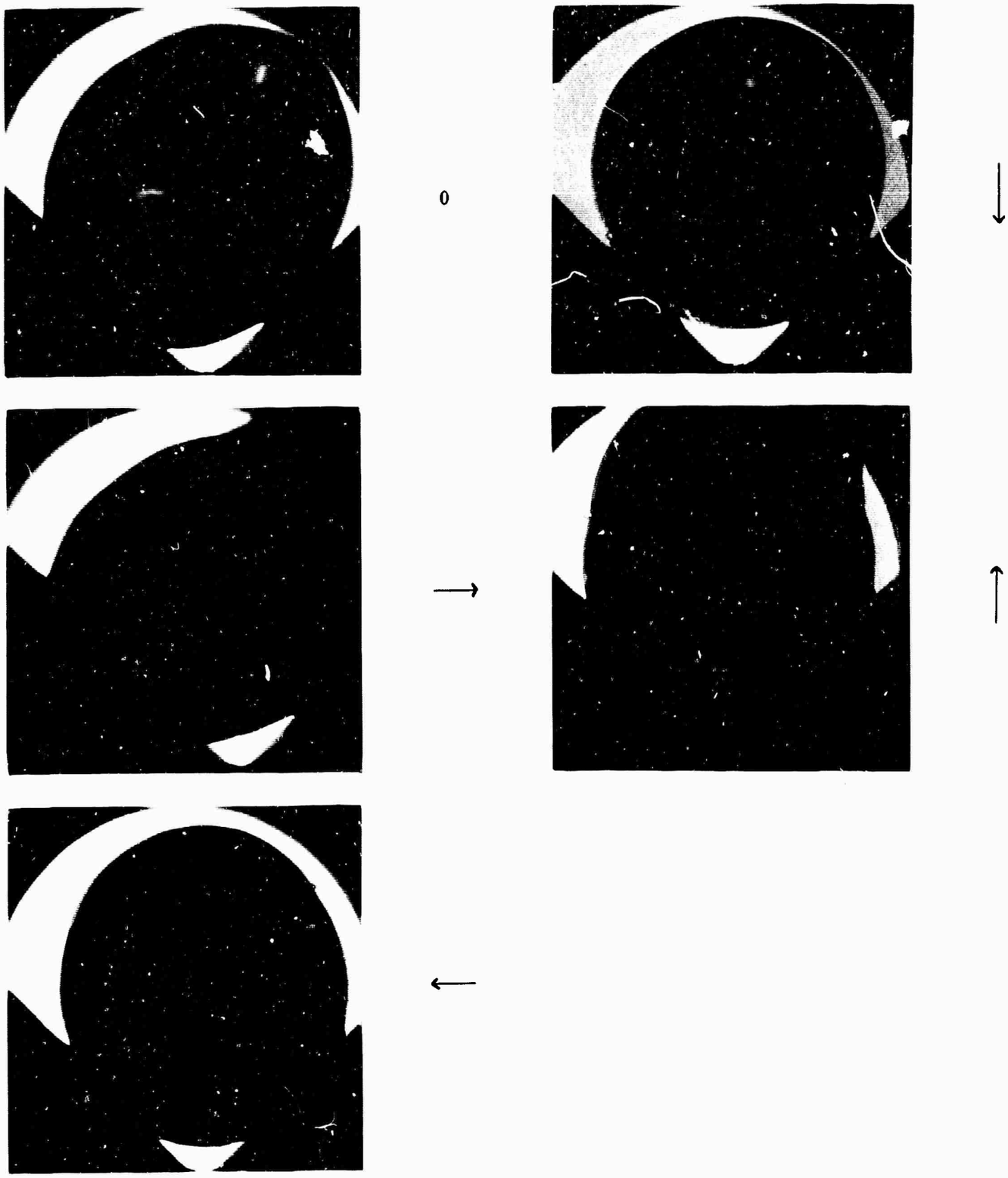

Figure 10. No. 2500-10-5 - Schlieren photograph showing the effect of horizontal and vertical movement of the boule on core shape and size.

conical interface found in ruby crystal, where all "r" plane facets with normals to the growth direction between approximately sixty degrees and zero are confined to the tip.

To separate the central cores on a schlieren photograph would require a relative movement between the top and bottom of the rod of about 0.5 mm; with a six-inch long rod, this represents an angle of approximately 10 minutes. It is suggested then that more consistency can be achieved over both the size and shape of the core if the laser rods are fabricated with faces normal to the growth direction to within an accuracy 10 minutes.

With our "sixty degree" orientation seed crystal, a second "r" plane occurs with a normal at 67° from the growth axis. Under present growth conditions, this plane is almost tangential to the growth interface and two facets are formed, one coming away from the tip and the other half way up the interface. The large angle cores are not so distinct as those confined to the center; however, because of their much larger relative size slight misorientations relative to the growth axis have a much more pronounced effect on the apparent core size and shape.

It has been shown that changes in the melt temperature can effectively change the conical angle of the growth interface. Because of the steep angle encountered with ruby and sapphire crystals, a relatively small change in temperature is sufficient to move the facet from the side to the tip of the interface when the angle between the "r" plane normal and the growth direction is around 65°. The temperature fluctuation is not enough to affect the quality of the boule but would most likely be reflected as a small change in the "as grown" diameter.

It can be shown that a change in seed orientation such as to move the angle between the "r_2" normal and the growth direction to a value greater than 70° will effectively remove the facet (and corresponding core) tangential to the growth interface. Using a seed of orientation such that growth direction is along the "r" plane normal would do this most effectively. A complication arises, however, due to the fact that there is a tendency for a crystal growth with this orientation to become elliptical and produce an elliptical shaped core; this can clearly be seen in Figure 3.

In addition to retaining a concentric boule throughout the growth cycle, it is also important that the crystal grows straight. The effect of not keeping the boule straight can be seen by examination of Figures 7 and 9. Boule No. 2500-33-16 was not perfectly straight and it was impossible to manipulate the orientation to produce one well defined core; this should be compared with Boule No. 2500-10-5 which has been grown from the same seed but was much straighter down its length.

This preliminary study has shown that the size and shape of the core in a fabricated laser rod is dependent on three factors:

(i) The growth orientation

(ii) The straightness and concentricity during growth

(iii) Misorientations during fabrication

The effect of growth orientations is becoming clear and work will proceed in order to reduce the core size. The use and better understanding of the shape monitoring device has in recent months improved both the straightness and concentricity of the as-grown boules. The improvement is such that contributions to the apparent core size and shape during the actual growth are relatively small compared to that introduced by small misorientations during fabrication. The effect of these misorientations could be minimized by lining up the rods, using the schlieren technique, to give minimum core size and fabricating the ends normal to the laser light beam.

In an attempt to determine the variation in chromium content across the core measurements have been made on polished windows using both the electron probe and spectrographic absorption techniques.

The electron probe work has not yet been completed and will be reported at a later date. Preliminary work using an optical absorption technique has indicated an increase in chromium content in the vicinity of the core. Figure 11 shows the result of scanning across the window using light polarized with $\vec{E}$ normal

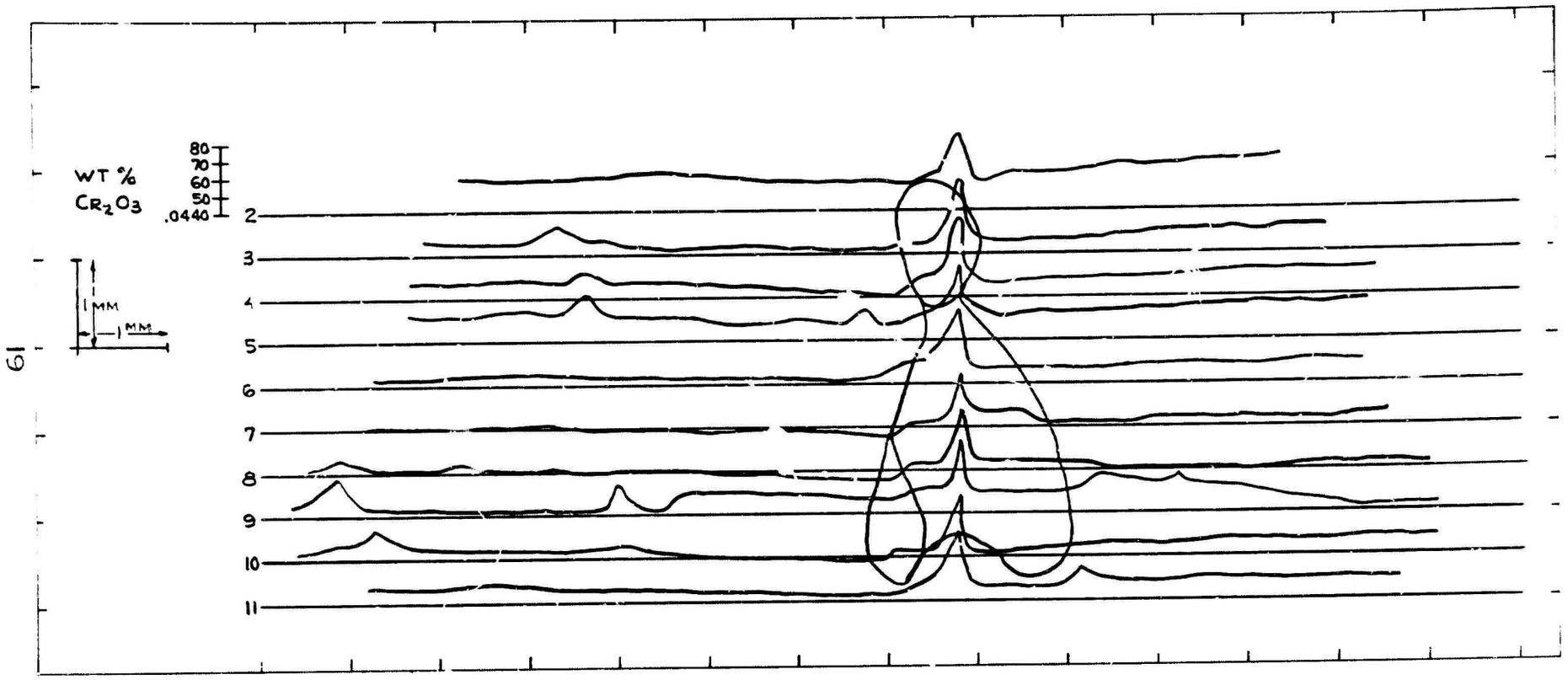

FIG. 11 OPTICAL ABSORPTION SCAN ACROSS A RUBY WINDOW TO DETERMINE THE CHROMIUM CONCENTRATION IN THE VICINITY OF THE CORE.

to the C axis. The scan was made along the direction shown on a schlieren photograph of the window in Figure 12. The base line for each scan shown in Figure 11 was taken as 0.0440 wt % Cr_2O_3, and the shape of the core shown on the diagram was copied directly from the schlieren photograph; the larger peaks are due to reference scratches on the surface.

It is possible to see a correlation between the core and a corresponding localized rise in chromium concentration. The increase is only about 3% and care has to be taken in proper alignment of the instrument as well as obtaining the optimum window thickness and surface finish. It is hoped that further refinement of the technique will lead to more conclusive results from future work.

In addition to finding out information concerning the origin and physical characteristics of the core, it is also important to know what is its influence on the active lasing properties of the ruby rod. Preliminary examination of the problem has shown that a possible association can exist between the core and an uneven energy distribution in the near field lasing pattern; it is also possible to correlate the schlieren patterns obtained under both active and passive testing.

To further this effort, a series of laser rods are presently being fabricated for testing in the laboratory's recently acquired Korad K2 Laser Head. These contain a number of different core structures obtained by changing the seed orientation and the corresponding facet formation at the interface; a comparison will be made between these rods and two others which have been selectively cut from a larger diameter ruby to be core free.

Figure 12. Schlieren of window used in optical absorption work; scan was made horizontally along the lines shown.

(2) Internal Laser Damage

The peak power obtainable from Q-switched laser systems is limited at this time chiefly by damage attributable to particulate inclusions. In the case of glass, it has been recognized for some time that platinum inclusions introduced during the melting process are at fault. It has been demonstrated that crucible material (iridium) inclusions led to damage in Czochralski rubies grown in the present program.[6] We have examined some of the Verneuil rubies damaged in laser studies by Avizonis and Farrington[7] and there too found evidence presented below that damage was related to inclusions.

The problem with platinum in glass and iridium in ruby is assumed to be that these inclusions absorb pump and laser radiation and thereby cause damage to the matrix by several possible routes ranging from expansion to fusion and perhaps vaporization of the inclusion, or perhaps by thermal stressing of the matrix. We have made calculations on various aspects of the heating of inclusions - specifically iridium - in an effort to clarify the damage mechanism, to point up more precisely the type of control against inclusions needed in the growth process and to indicate what experimental observations in damage testing may be fruitful. These calculations are summarized in Section (b) below, following a presentation of damage threshold data, including Czochralski ruby results, in Section (a).

(a) Damage Threshold Data

The damage threshold data of Avizonis and Farrington[7] are represented in Figure 13 by the circled points showing experimental scatter. The

---

(6) "Czochralski Ruby", Report No. SRCR-66-2 by F. R. Charvat, O. H. Nestor, and J. C. Smith, Union Carbide Corporation, Linde Division, Speedway Laboratories, January 26, 1966. (Semi-annual Technical Summary Report, Contract NONr-4132(00).

(7) P. V. Avizonis and T. Farrington, Internal Self-Damage of Ruby and Nd-Glass Lasers, Appl. Phys. Letters 7 (8), 205 (15 October 1965).

curves drawn through these points are not those of Avizonis and Farrington. Rather, the curves drawn here - particularly that for ruby - point up a new summary of the results, viz. that the damage threshold is energy-limited at the shortest pulse lengths, but power-limited at longer (> 50 nanoseconds). How far the power limit may extend is clearly not defined. It presumably does not extend into the millisecond pulse length regime with the same power limits indicated in Figure 13 (300 megawatts/cm^2 for ruby and 120 megawatts/cm^2 for glass) for then the damage thresholds at 1 milliseconds would be 300 Kilojoules/cm^2 and 120 Kilojoules/cm^2, respectively, for ruby and glass. The latter is ca. 600x greater than the value reported by Avizonis and Farrington.

Figure 13 shows two other points - one for a Czochralski ruby designated by an open square and the other for a Verneuil ruby denoted by a full square - representing the results of other, more recent tests at Kirtland AFB[8] conducted to update the Czochralski-Verneuil comparison. Like the other points, these represent the onset of damage at the output end of amplifier rods. The pulse length assignment is nominal. The discrepancy between the new Verneuil rod and the others defining the full curve is not resolvable except in speculation. The new Verneuil rod and the Czochralski rod were remarkably similar in damage behavior. Each was damaged also at its input end in a manner similar to that shown in Figure 1 of Reference (6). That type of damage has been assumed to be a focusing - rather than an inclusion - induced effect, because the damage location is highly reproducible and the form of damage rather unique.

---

(8) We gratefully acknowledge the cooperation of the Effects Branch of the AF Weapons Laboratory, Kirtland AFB, New Mexico, in testing rods for damage and in particular the helpful efforts of Dr. P. V. Avizonis, Capt. K. C. Jungling, and Sgt. W. Willoughby.

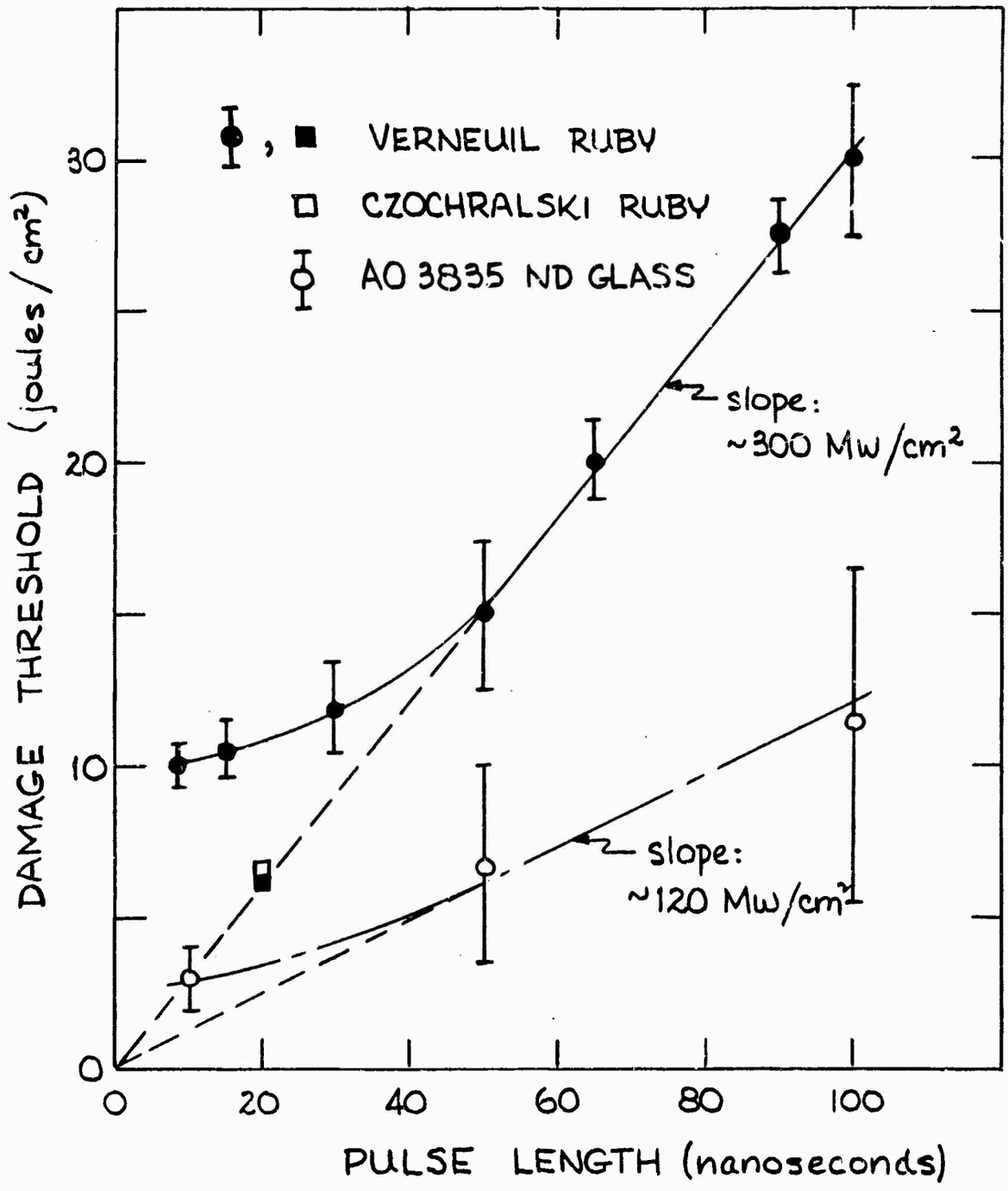

Figure 13. Energy Threshold for Laser Internal Damage vs Pulse Length

Avizonis and Farrington have noted that there was no damage observable due to pump light (u-v filtered out) even with pump energies higher than normally used. [7]

We have examined some of the Verneuil rubies damaged in their work. We succeeded in splitting open one of the rubies at and along a damage center "plane". X-ray studies identified this as an r-plane (10 · 1) and an electron microprobe survey of the damage zone disclosed a multiplicity of particles, each containing nickel, iron and chromium and ranging in size up to about 40 microns. [9] These were comparable in size to opaque inclusions spotted in other damage zones in the same crystal. The stainless steel "debris" indicated by the electron probe studies is assumed to have been in metallic form inasmuch as it appeared to be related to inclusions that are opaque and since it was entrapped during growth under reducing conditions.

(b) Heating of Inclusions

The data of Figure 13 invite interpretation as follows:

1. The energy threshold limit as pulse length approaches zero reflects what is needed to produce damage when inclusions do not lose thermal energy to their environment. The energy threshold for Czochralski ruby is shown below to be sufficient to bring iridium inclusions, as identified thus far, to melting, if re-radiation from the inclusion and conduction cooling are neglected. Re-radiation is in fact entirely negligible. It is assumed that conduction cooling is negligible in the short times involved.

2. The energy threshold increases with pulse length as a result of energy exchange from inclusion to the matrix. The exchange mechanism,

---

(9) We are indebted to Mr. A. M. Hawley of our Laboratories for the X-ray work and to Dr. W. D. Forgeng and his staff members. Mrs. Gloria M. Faulring, and Mr. E. S. Malizie, of the Union Carbide Mining and Metals Division, Technology Department, Niagara Falls, New York, for the electron probe work.

if thermal, must be conduction. On this assumption, it is shown that temperatures of ca. 6000°K may be generated at the inclusion site during a laser pulse. But it also follows that the thermal gradients calculated are so excessive as to make the classical treatment of conduction suspect.

The purpose of this section is to describe the calculations supporting the above comments. The calculations are made with specific reference to iridium inclusions, since something of their size, shape and orientation is known. Iridium inclusions are taken to be platelets, as reported in Reference (6). Only laser radiation is included as a heat source, in light of the Avizonis and Farrington finding that the pump source produces no damage.

Symbols to be used are defined as follows:

s = platelet thickness, cm

ℓ = platelet breadth, cm

a = broad area of platelet cm^2

A = total surface area of platelet, cm^2

θ = angle between platelet normal and laser beam

ρ = density, gm/cm^3

C = specific heat, joules/gm-°K

e_λ = spectral emissivity at laser

e_T = total emissivity

T = temperature, °K

E = laser pulse energy "density", $joules/cm^2$

τ = laser pulse length, seconds

σ = Stefan-Boltzman constant

$= 5.67 \times 10^{-12}$ $watts/cm^2\text{-}deg^4$

t = time, seconds

The subscript "$_o$" will be used to denote the matrix.

(i) Energy Threshold Limit

It will be shown that the damage threshold given in Figure 13 for Czochralski ruby is of the order needed to heat iridium inclusions to melting. The heat energy needed to melt iridium is 1.2×10^4 joules per cm^3 including the heat of fusion (see Table 2 below). Then the energy needed for a platelet of broad area a and thickness s is $1.2 \times 10^4 a$ s. The energy absorbed by the platelet from a beam of energy flux density E is $e_\lambda a \cos\theta E$. The flux density E_m needed to produce melting is then given by

$$e_\lambda a \cos\theta E_m = 1.2 \times 10^4 a s$$

or

$$E_m = \frac{1.2 \times 10^4 s}{e_\lambda \cos\theta} \qquad (1)$$

For iridium, $e_\lambda = 0.3$ at the Cr R-line in ruby.[10] The platelets are presumed to have been pulled into the melt by the convection currents therein. It is assumed that the platelet then adheres to the growth interface and hence is oriented in the ruby according to the geometry of the interface. The latter is typically conical with a cone angle of 45° included. Thus, $\theta \sim 67°$ and $\cos\theta \sim 0.4$. Then

$$E_m = 10^5 s. \qquad (2)$$

In Reference (6), it was noted that iridium inclusions were of the order of 10 microns ($= 10^{-3}$ cm) across, on the average, and that the breadth to width ratio was roughly $\ell/s \sim 20$. Hence, $s \sim .5$ microns $= 5 \times 10^{-5}$ cm and

$$E_m \sim 5 \text{ joules/cm}^2$$

This is comparable to the damage threshold value for Czochralski ruby given in Figure 13.

---

(10) AIP Handbook, Table 6k-5, 2nd Ed. (McGraw-Hill Book Company, Inc.).

It should be clear that too many factors - such as laser beam intensity distribution, inclusion sizes, and the like - are not well enough defined to allow pinpointing the damage criterion to the actual melting of iridium inclusions or to heating them to the melting point of sapphire or any other specific point at this time. But it does appear that significant heating of inclusions is necessary to produce damage.

It is assumed that a similar result applies rather generally, i.e., to Verneuil ruby and its inclusions and to platinum in glass, in the range of laser operating conditions considered here. It is of interest to compare the various metallic inclusions as to the energy needed to bring an inclusion of given volume to melting. This is done in Table 2 where the energy needed to heat an inclusion to the melting point of sapphire (2310°K is also listed).

TABLE 2

Heat Content ΔH above 273°K[11]

Element	M. P. (°K)	ΔH (joules/cm³) To Melting	Melted	To 2310°K
Nickel	1730	7250	9900	13100
Iron	1800	7850	9900	12300
Chromium	2160	9070	11300	12200
Platinum	2030	5860	8300	>8300
Iridium	2450	9200	12100 *	7320
Tungsten	3640	----	-----	6100

It is apparent that iridium is more or less preferred over transition metal inclusions depending on whether melting of the inclusions is more important than approaching the melting point of the matrix. In either case the factor of difference would be no more than 2x. Table 2 also shows platinum at a disadvantage by virtue of low heat requirement; and, if the lower melting point of glass as opposed to sapphire makes itself felt, then it is clear that damage thresholds should be lower for Pt in glass.

(11) Calculated from data compiled by K. K. Kelley. Bulletin 371, Bureau of Mines, Dept. of Commerce, and from AIP Handbook data where denoted by * .

All these attempts to compare different materials are based on equal sizes of inclusions. In an experimental comparison the size, shape, and orientation of inclusions must be taken into account. Inasmuch as these factors are generally unknown for laser materials and in particular those of Figure 13, close correlation of threshold data with the kind of calculation given above cannot be made at this time.

Eq. (1) points up the fact that the thickness of inclusions is the important size parameter determining damage threshold (similarly, for spherical inclusions, $E_m \sim r$, the inclusion radius.) The first damage would occur to the thinnest (smallest) inclusions and as laser radiation increases in intensity progressively larger inclusions are damaged. This has several implications:

(1) Growth procedures that simply reduce the size of inclusions are ill-founded.

(2) Damage threshold differences between individual rods are a matter not only of the number density of inclusions but also of the size range in the manner noted above.

An apparent increase in the size of damage sites with increased laser output may prove on closer inspection to be the formation of new, larger damage sites.

(ii) Heat Losses from Inclusions

In the above discussion heat losses from the inclusion have been neglected. We will now consider these for the case of iridium in ruby.

The rate at which an inclusion re-radiates energy is given by $C_T \sigma A(T^4-T_o^4)$. The ratio of this to the average heating rate e_λ acosΘ E/τ is:

$$R = \frac{A}{a \cos \Theta} \cdot \frac{e_T}{e\lambda} \cdot \frac{\sigma(T^4-T_o^4)}{E/\tau} \qquad (3)$$

(For spherical inclusions the ratio A/a cos Θ is replaced by A/a = 2.)

For platelets, $A/a \sim 2$, and, in the case of iridium in Czochralski ruby, $\cos \Theta \sim 0.4$, so that $A/a \cos \Theta \sim 5$. With $e_\lambda \sim 0.3$, $E/\tau = 300$ Mw/cm^2 = 3 x 10^8 watts/cm^2 (Figure 13) and neglecting T_o^4 relative to T^4:

$$R \sim 5 \times 10^{-8} e_T \sigma T^4$$

R equals unity for a black body ($e_T = 1$) at T = 42000°K! Hence, R << 1 typically.

At a nominal value of $E/\tau = 10^4$ watts/cm^2 and with $e_T = 0.3$ (as is the case for a variety of metals at T ~ 2500°K),

$$R \sim 3 \times 10^{-15} T^4$$

At the melting point of iridium ($T \sim 2.7 \times 10^3$ °K), $R \sim 1/6$. Thus even in this low laser power case, radiation cooling is quite negligible.

The only thermal cooling mechanism that can be of any consequence is conduction in the ruby material. What we have considered here is a simplified problem in which the inclusion is neglected except as it serves the intermediary function of making the laser energy it absorbs available to the ruby. Specifically, the energy is absorbed at rate

$$I = e_\lambda \, a \cos \Theta \, E/\tau \qquad (4)$$

and is delivered to the matrix over area a. Considering a one-dimensional heat flow treatment to be justified by the short pulse times encountered, the temperature at

distance X from the inclusion plane is given by [12]:

$$T(x,t) = \frac{I}{a}\frac{\sqrt{a_o t}}{\kappa_o}\left[\frac{e^{-u^2}}{\sqrt{\pi}} - u\,\mathrm{erfc}\,u\right] \qquad (5)$$

where $u = X/(2\sqrt{a_o t})$, a_o = thermal diffusivity of sapphire = $\kappa_o/(\rho_o c_o)$, and κ_o, ρ_o, c_o are the thermal conductivity, density and specific heat of sapphire, respectively. This solution assumes temperature independent thermal properties of the matrix, which is not valid, but here it is used for simplicity and will be compensated for in part by assuming average values. Using now Eq. (4) and $e_\lambda = 0.3$, $\cos\Theta = 0.4$, $\rho_o = 4$, the temperature at x = 0 (the "surface", or plane of iridium - sapphire contact) is

$$T(o,\ t) = 0.034\,\frac{E}{\tau}\sqrt{\frac{t}{c_o \kappa_o}}$$

The median value of the product $c_o \kappa_o$ over the range 273-2000°K is about 0.2 cgs; this will be used below. The "surface" temperature at the end of the pulse time $t = \tau$ for average laser power of $E/T = 3 \times 10^8$ watt/cm^2 is then

$$T(o, \tau) \sim 2 \times 10^7 \sqrt{\tau}$$

For τ = 70 nanosec = 7×10^{-8} sec, in the middle of the range covered in Figure 13,

$$T(o, \tau) \sim 6000°K$$

in excess of the boiling point of sapphire. This result is not taken literally, but again is indicative of the need for generating high temperatures to produce damage.

The above treatment of the conduction problem gives some cause for concern inasmuch as the implied temperature gradient at the "surface" is approximately 10^8 °K/cm., or 10°K per unit hexagonal cell (6 Al_2O_3 molecules) of sapphire. This is so large as to virtually violate the temperature concept, making the classical heat conduction treatment high tenuous.

---

(12) H. S. Carslaw and J. C. Jaeger "Conduction of Heat in Solids", Clarendon Press, Oxford (1959), 2nd Ed., p. 262-3.

In summary, the above calculations support the assumption that inclusion heating via laser beam absorption is in fact involved in the ruby damage mechanism, and they suggest that heating to temperatures as high as, or higher than, the melting point of the inclusion, or of sapphire, is characteristic. They further point up the fact that damage sets in sooner - i.e. thresholds are lowered - as inclusion size decreases.

Recent experimental data [13] has further indicated the importance of the particle size on laser damage. A 1/4-inch diameter by 3-inch long ruby laser rod evaluated to have a considerable number of inclusions was lased and examined for damage after successive testing at an input energy of 125 joules.

A correlation was attempted between the observed damage sites and inclusions in the crystal which had been carefully mapped out prior to testing. Similar to what had been reported previously[6], the number of damage sites far exceeded the number of visible inclusions; no damage, however, was observed at any of the previously spotted inclusions.

Examination of polished windows cut from ruby boules under dark and bright field illumination on a Zeiss Universal Microscope has shown a large variation in particle size. A small number of inclusions are in the size range between 10-30 microns with the majority less than 10 microns. In the lasing experiment described above, the crystal was examined under low power in order to be able to scan over the entire length. Under these circumstances, only the larger inclusions would be visible; the majority of inclusions which were smaller and more likely to be damaged remained undetected during the initial examination.

No correlation was possible between theory and experiment as no measurements were made on the actual particle size; it is also possible that some particles below the level of detection for the microscopic technique used were still too large to contribute to laser damage at these input energy levels.

---

(13) We are indebted to L. R Rothrock of our Laboratory for carrying out these lasing experiments.

(3) Large Ruby Growth

A furnace has been constructed to house a 5,000 cc iridium crucible. The basic design of the furnace is similar to that used in the growth of smaller diameter boules with necessary modifications to allow for the larger heat capacity of the system and the increased weight of the crucible plus charge load. Considerable plastic flow occurs in iridium at operating temperatures, and the problem of providing the crucible with adequate support to prevent sagging of the sides and bottom had to be investigated closely. Also requiring attention was an investigation into correct combination of coil design and furnace insulation in order to come up with the most efficient heating conditions; this was done by coupling directly into the empty crucible and measuring the temperature as a function of coil diameter, number of turns, and thickness of furnace insulation. This work was necessary because the power level of the available generator was slightly low and care had to be taken to avoid drawing plate current in excess of the rated maximum. This information having been accumulated, a melt was established and a series of experiments carried out to establish the conditions for forming a suitable temperature distribution from which a crystal could be seeded.

The first growth was carried out under conditions which were far from ideal and the crystalline quality was poor. However, the size was correct and a considerable amount of valuable experience was gained from the exercise; the crystal is shown in Figure 14.

The main problem associated with this initial growth was in temperature control where matching was not achieved between the heat capacity of the system to the correct controller setting. The response of this system was much slower than normally encountered, and growth rate fluctuations arising from excessive temperature cycling of the melt temperature resulted in poor crystalline quality.

After modification of the control system, a second crystal was grown which was much improved both in shape and quality of the resultant boule. However, the improvement in quality created problems in the power requirements for growth. Because of the improved quality, more radiant heat was removed along the length of the crystal and more power was required from the generator in order to maintain growth. The combined effect of running the generator closer to its maximum rated power and an arcing problem at one of the input leads resulted in a shutdown towards the end of the growth cycle. Cracking occurred in the crystal due to the necessity of having to remove it too rapidly from the solidifying melt.

Modification of the RF generator was carried out to raise its operational power level and a third crystal grown. For this experiment, additional shielding was incorporated above the crucible and the crystal cooled over a very much longer period of time to eliminate thermal stressing. Also at this point, enough confidence was felt in both our ability and technique to employ the method routinely used on smaller diameter crystals for the reduction of iridium inclusions[6].

Figure 15 shows the "as grown" boule containing 0.05 wt % Cr_2C_3. The quality is good throughout except where a diameter change led to a drop in growth rate with a resulting nucleation of bubbles at the interface.

An examination of the boules, using the standard technique of shining a well collimated beam of light into the crystal and viewing the scattered radiation, failed to detect any inclusions. It is possible that some inclusions are present and remained undetected because the light intensity was lower than required for so large a boule; it is not expected, however, that the number exceeds that specified as being acceptable for present day ruby laser crystal requirements.

To adequately pump a ruby rod of dimensions 2 inches in diameter and 12 inches long, the chromium concentration must not exceed 0.013 weight percent Cr_2O_3[14]; thus the latest large diameter crystal produced

---

(14) V. O. Nicolai, private communication.

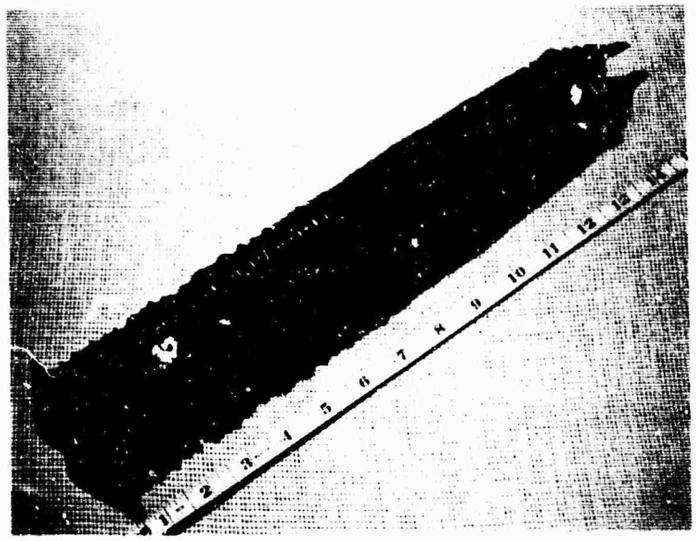

Figure 14. Large diameter ruby boule containing 0.05 wt % Cr_2O_3 - first growth.

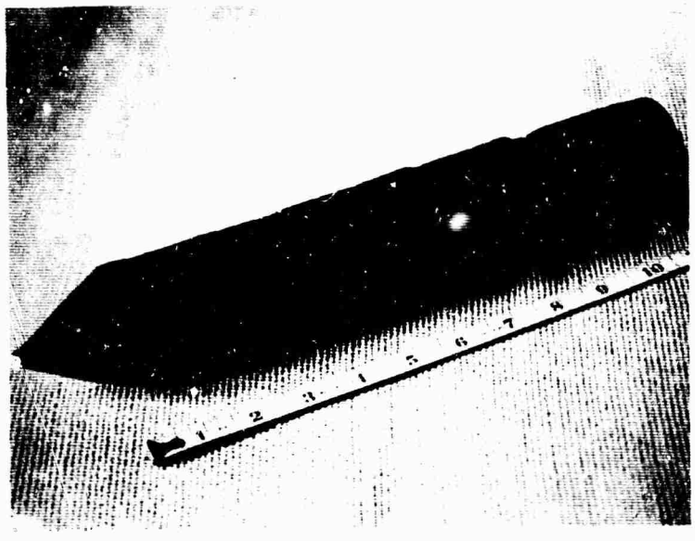

Figure 15. Large diameter ruby boule containing 0.05 wt % Cr_2O_3 - third growth.

under the present contract has been grown specifically with this concentration. This crystal will be fabricated with inspection ends to examine its optical quality.

Having overcome the technical problems of growing so large a single crystal of good quality, future work will be devoted to improving further the optical quality; this in turn will require modification of our present optical evaluation techniques which have been set up to accommodate crystals of somewhat smaller diameter.

III. PLANS FOR NEXT PERIOD

Future plans are for essentially a continuation of our present effort.

The effect of chromium distribution on active lasing will be investigated in more detail. This work will be complemented by an equivalent study of the core origin and how its effect can be minimized or eliminated by suitable refinement of our existing growth process.

Results indicate that the size of the inclusions is an important factor. Both the effect of modifying the growth technique and purification of the starting raw material on the size and distribution of inclusions will be investigated; a parallel study will again be carried out on the effect of these changes on laser damage during active testing.

The optical quality of the large diameter crystal will be evaluated and the necessary modifications made to the growth process in order to achieve the same high standard which is at present obtained with smaller diameter boules.

1	0042	H. CUMMINGS	54	*
2	0042	JOHNS HOPKINS UNIVERSITY	54	
3	0042	BALTIMORE, MARYLAND 21218	54	
1	0121	T. C. MACAVOY	54	*
2	0121	CORNING GLASS WORKS	54	
3	0121	CORNING, NEW YORK 14832	54	
1	0139	O. H. NESTOR	54	*
2	0139	LINDE COMPANY	54	
3	0139	1500 POLCO STREET	54	
4	0139	INDIANAPOLIS, INDIANA 46222	54	
1	0189	J. W. TURNER	54	
2	0189	WESTINGHOUSE ELECTRIC CORP.	54	
3	0189	ELECTRONICS DIVISION	54	
4	0189	P. O. BOX 1897	54	
5	0189	BALTIMORE, MARYLAND 21203	54	
1	0207	R. W. YOUNG	54	
2	0207	AMERICAN OPTICAL COMPANY	54	
3	0207	SOUTHBRIDGE, MASSACHUSETTS /UKK/	54	
1	0213	DR. JERALD R. IZATT	54	*
2	0213	NEW MEXICO STATE UNIVERSITY	54	
3	0213	UNIVERSITY PARK, NEW MEXICO 88070	54	
1	0216	MR. CHARLES G. NAIMAN	54	*
2	0216	MITHRAS, INC.	54	
3	0216	CAMBRIDGE, MASSACHUSETTS 02138	54	
1	0218	DR. JACK A. SOULES	54	
2	0218	PHYSICS DEPARTMENT	54	
3	0218	NEW MEXICO STATE UNIVERSITY	54	
4	0218	UNIVERSITY PARK, NEW MEXICO 88070	54	
1	0220	PHYSICAL SCIENCES DIVISION	54	
2	0220	ARMY RESEARCH OFFICE	54	
3	0220	OFFICE, CHIEF, RESEARCH & DEVELOPMENT	54	
4	0220	WASHINGTON, D. C. 20360	54	
5	0220	ATTN DR. ROBERT A. WATSON	54	
1	0221	CHIEF SCIENTIST	54	
2	0221	U. S. ARMY ELECTRONICS COMMAND	54	
3	0221	FORT MONMOUTH, NEW JERSEY 07703	54	
4	0221	ATTN DR. HANS K. ZIEGLER	54	
1	0222	DIRECTOR, INSTITUTE FOR EXPLATORY RESEARCH	54	
2	0222	ARMY SIGNAL RESEARCH&DEVELOPMENT LABORATORY	54	
3	0222	FORT MONMOUTH, NEW JERSEY 07703	54	
1	0223	ASST DIRECTOR OF SURVEILLANCE	54	
2	0223	ARMY SIGNAL RESEARCH&DEVELOPMENT LABORATORY	54	
3	0223	FORT MONMOUTH, NEW JERSEY 07703	54	
4	0223	ATTN DR. HARRISON J. MERRILL	54	

1	0236	OFFICE, AEROSPACE RESEARCH /MROSP/		54
2	0236	WASHINGTON, D. C. 20360		54
3	0236	ATTN LT. COL. IVAN ATKINSON		54
1	0238	TECHNICAL AREA MANAGER /760A/		54
2	0238	ADVANCED WEAPONS AERONAUTICAL SYSTEMS DIV		54
3	0238	WRIGHT-PATTERSON AFB		54
4	0238	OHIO 45433		54
5	0238	ATTN MR. DON NEWMAN		54
1	0239	PROJECT ENGINEER /523T/		54
2	0239	AEROSPACE RADIATION WEAPONS		54
3	0239	AERONAUTICAL SYSTEMS DIVISION		54
4	0239	WRIGHT-PATTERSON AFB		54
5	0239	OHIO 45433		54
6	0239	ATTN MR. DON LEWIS		54
1	0240	AIR FORCE SPECIAL WEAPONS CENTER /SWRPA/		54
2	0240	KIRTLAND AFB		54
3	0240	NEW MEXICO 87117		54
4	0240	ATTN MAJOR T. T. DOSS		54
1	0241	PROJECT ENGINEER /5561/ COMET		54
2	0241	ROME AIR DEVELOPMENT CENTER		54
3	0241	GRIFFISS AFB		54
4	0241	NEW YORK 13442		54
5	0241	ATTN MR. DURWOOD CREED		54
1	0242	DEPARTMENT OF ELECTRICAL ENGINEERING		54
2	0242	NEW YORK UNIVERSITY		54
3	0242	UNIVERSITY HEIGHTS		54
4	0242	NEW YORK, NEW YORK 10003		54
5	0242	ATTN MR. THOMAS HENION		54
1	0243	BMDR	8 COPIES	54
2	0243	ROOM 2 B 263		54
3	0243	THE PENTAGON		54
4	0243	WASHINGTON, D. C. 20301		54
5	0243	ATTN MAJOR GLENN SHERWOOD		54
1	0284	MR. JOHN EMMETT		54
2	0284	PHYSICS DEPARTMENT		54
3	0284	STANFORD UNIVERSITY		54
4	0284	PALO ALTO, CALIF. 94305		54
1	0326	SECRETARY, SPECIAL GROUP ON OPTICAL MASERS	3 COPIES	54
2	0326	ODDRCE ADVISORY GROUP ON ELECTRON DEVICES		54
3	0326	346 BROADWAY - 8TH FLOOR		54
4	0326	NEW YORK, NEW YORK 10013		54
1	0352	ASD /ASRCE-31/		54
2	0352	WRIGHT-PATTERSON AFB, OHIO 45433		54
1	0372	TECHNICAL AREA MANAGER /760B/		54
2	0372	SURVEILLANCE ELECTRONIC SYSTEMS DIVISION		54
3	0372	L. G. HANSCOM AFB		54
4	0372	MASSACHUSETTS 01731		54
5	0372	ATTN MAJOR H. I. JONES, JR.		54

1	0388	COMMANDING OFFICER		54
2	0388	U. S. NAVAL ORDNANCE LABORATORY		54
3	0388	CORONA, CALIF. 91720		54
1	0420	DIRECTOR		54
2	0420	U. S. ARMY ENGINEERING RESEARCH		54
3	0420	AND DEVELOPMENT LABORATORIES		54
4	0420	FORT BELVOIR, VIRGINIA 22060		54
5	0420	ATTN TECHNICAL DOCUMENTS CENTER		54
1	0449	OFFICE OF THE DIRECTOR OF DEFENSE	2 COPIES	54
2	0449	DEFENSE RESEARCH AND ENGINEERING		54
3	0449	INFORMATION OFFICE LIBRARY BRANCH		54
4	0449	PENTAGON BUILDING		54
5	0449	WASHINGTON, D. C. 20301		54
1	0471	U. S. ARMY RESEARCH OFFICE	2 COPIES	54
2	0471	BOX CM, DUKE STATION		54
3	0471	DURHAM, NORTH CAROLINA 27706		54
1	0499	DEFENSE DOCUMENTATION CENTER	20 COPIES	54
2	0499	CAMERON STATION BUILDING		54
3	0499	ALEXANDRIA, VIRGINIA 22314		54
1	0527	DIRECTOR	6 COPIES	54
2	0527	U. S. NAVAL RESEARCH LABORATORY		54
3	0527	TECHNICAL INFORMATION OFFICER		54
4	0527	CODE 2000, CODE 2021		54
5	0527	WASHINGTON, D. C. 20390		54
1	0555	COMMANDING OFFICER		54
2	0555	OFFICE OF NAVAL RESEARCH BRANCH OFFICE		54
3	0555	219 S. DEARBORN ST.		54
4	0555	CHICAGO, ILLINOIS 60604		54
1	0584	COMMANDING OFFICER		54
2	0584	OFFICE OF NAVAL RESEARCH BRANCH OFFICE		54
3	0584	207 W. 24TH ST.		54
4	0584	NEW YORK, NEW YORK 10011		54
1	0640	COMMANDING OFFICER		54
2	0640	OFFICE OF NAVAL RESEARCH BRANCH OFFICE		54
3	0640	1076 MISSION STREET		54
4	0640	SAN FRANCISCO, CALIFORNIA 94109		54
1	0696	AIR FORCE OFFICE OF SCIENTIFIC RESEARCH		54
2	0696	WASHINGTON, D. C. 20333		54
1	0724	DIRECTOR		54
2	0724	NATIONAL BUREAU OF STANDARDS		54
3	0724	WASHINGTON, D. C. 20234		54
1	0752	DIRECTOR		54
2	0752	RESEARCH DEPARTMENT		54
3	0752	U. S. NAVAL ORDNANCE LABORATORY		54
4	0752	WHITE OAK, SILVER SPRING, MD. 20910		54

1	0780	COMMANDING OFFICER	54
2	0780	OFFICE OF NAVAL RESEARCH BRANCH OFFICE	54
3	0780	1030 EAST GREEN STREET	54
4	0780	PASADENA, CALIFORNIA 91101	54
1	0808	COMMANDING OFFICER	54
2	0808	OFFICE OF NAVAL RESEARCH BRANCH OFFICE	54
3	0808	495 SUMMER STREET	54
4	0808	BOSTON, MASS. 02210	54
1	0836	U. S. NAVAL RADIOLOGICAL DEFENSE LABORATORY	54
2	0836	/CODE 941/	54
3	0836	SAN FRANCISCO, CALIFORNIA 94135	54
1	0853	COM' NDING OFFICER	54
2	0853	U. S. ARMY MATERIALS RESEARCH AGENCY	54
3	0853	ATTN TECHNICAL LIBRARY	54
4	0853	WATERTOWN, MASSACHUSETTS 02172	54
1	0875	BOULDER LABORATORIES	54
2	0875	NATIONAL BUREAU OF STANDARDS	54
3	0875	ATTN LIBRARY	54
4	0875	BOULDER, COLORADO 80301	54
1	0918	AIR FORCE WEAPONS LABORATORY	54
2	0918	ATTN GUENTHER WLRPF	54
3	0918	KIRTLAND AIR FORCE BASE	54
4	0918	NEW MEXICO 87117	54
1	0932	CHIEF, BUREAU OF NAVAL WEAPONS	54
2	0932	DEPARTMENT OF THE NAVY	54
3	0932	WASHINGTON, D. C. 20360	54
4	0932	ATTN J. M. LEE RMGA-81	54
1	0976	AIR FORCE CAMBRIDGE RESEARCH LABORATORIES	54
2	0976	ATTN CRXL-R, RESEARCH LIBRARY	54
3	0976	LAWRENCE G. HANSCOM FIELD	54
4	0976	BEDFORD, MASSACHUSETTS 01731	54
1	0988	BATTELLE MEMORIAL INSTITUTE	54
2	0988	505 KING AVENUE	54
3	0988	COLUMBUS, OHIO 43201	54
4	0988	ATTN BMI-DEFENDER	54
1	1030	HEADQUARTERS, USAELRDL	54
2	1030	FORT MONMOUTH, NEW JERSEY 07703	54
3	1030	ATTN SELRA/SAR,NO-4, X, AND PF	54
1	1032	COMMANDER, U. S. NAVAL ORDNANCE TEST STATION	54
2	1032	CHINA LAKE, CALIF 93556	54
3	1032	ATTN MR. G. A. WILKINS /CODE 4041/	54
1	1039	PROF. RUBIN BRAUNSTEIN	54 *
2	1039	UNIVERSITY OF CALIFORNIA	54
3	1039	DEPARTMENT OF PHYSICS	54
4	1039	LOS ANGELES, CAL. 90007	54

1	1040	N. I. ADAMS	54	*
2	1040	PERKIN-ELMER CORP.	54	
3	1040	NORWALK, CONN. 06852	54	
1	1047	PROF. H. G. HANSON	54	*
2	1047	UNIVERSITY OF MINNESOTA	54	
3	1047	DULUTH, MINN. 55812	54	
1	1048	P. SCHAFFER	54	*
2	1048	LEXINGTON LABORATORIES, INC.	54	
3	1048	84 SHERMAN ST.	54	
4	1048	CAMBRIDGE, MASS. 02140	54	
1	1053	W. PRINDLE	54	*
2	1053	AMERICAN OPTICAL COMPANY	54	
3	1053	14 MECHANIC ST.	54	
4	1053	SOUTHBRIDGE, MASS. 01551	54	
1	1054	DR. ALAN HAUGHT	54	*
2	1054	PLASMA PHYSICS	54	
3	1054	UNITED AIRCRAFT CORP.	54	
4	1054	EAST HARTFORD, CONN. 06027	54	
1	1056	PROF. R. J. COLLINS	54	*
2	1056	UNIVERSITY OF MINNESOTA	54	
3	1056	DEPARTMENT OF ELECTRICAL ENG.	54	
4	1056	MINNEAPOLIS, MINN. 55455	54	
1	1057	DR. ALAN KOLB	54	*
2	1057	U. S. NAVAL RESEARCH LAB.	54	
3	1057	WASHINGTON, D. C. 20390	54	
1	1059	PROF. ARTHUR SCHAWLOW	54	*
2	1059	STANFORD UNIVERSITY	54	
3	1059	STANFORD, CALIFORNIA 94305	54	
1	1065	RESEARCH MATERIALS INFORMATION CENTER	54	
2	1065	OAK RIDGE NATIONAL LABORATORY	54	
3	1065	POST OFFICE BOX X	54	
4	1065	OAK RIDGE, TENN. 37831	54	
5	1065	ATTN MR. T. F. CONNOLLY	54	
1	1066	J-5 PLANS AND POLICY DIRECTORATE	54	
2	1066	JOINT CHIEFS OF STAFF	54	
3	1066	REQUIREMENTS AND DEVELOPMENT DIVISION	54	
4	1066	ATTN SPECIAL PROJECTS BRANCH	54	
5	1066	ROOM 2D982, THE PENTAGON	54	
6	1066	WASHINGTON, D. C., 20301	54	
1	1067	ADVANCED RESEARCH PROJECTS AGENCY	54	
2	1067	RESEARCH AND DEVELOPEMENT FIELD UNIT	54	
3	1067	APO 143, BOX 41	54	
4	1067	SAN FRANCISCO, CALIF. 94101	54	

1	1068	ADVANCED RESEARCH PROJECTS AGENCY	54	
2	1068	RESEARCH & DEVELOPMENT FIELD UNIT	54	
3	1068	APO 146, BOX 271	54	
4	1068	SAN FRANCISCO, CALIFORNIA 94101	54	
5	1068	ATTN MR. TOM BRUNDAGE	54	
1	1082	AIR FORCE MATERIALS LABORATORY	54	
2	1082	AIR FORCE SYSTEMS COMMAND	54	
3	1082	WRIGHT-PATTERSON AIR FORCE BASE, OHIO 45433	54	
4	1082	ATTN MAAM /LT. JOHN H. ESTESS/	54	
1	1084	PROF. DONALD S. MCCLURE	54	*
2	1084	INSTITUTE FOR THE STUDY OF METALS	54	
3	1084	UNIVERSITY OF CHICAGO	54	
4	1084	CHICAGO, ILLINOIS 60637	54	
1	1085	DR. DANIEL GRAFSTEIN	54	*
2	1085	GENERAL PRECISION, INC.	54	
3	1085	AEROSPACE GROUP	54	
4	1085	LITTLE FALLS, NEW JERSEY 07424	54	
1	1087	DR. R. C. LINARES	54	*
2	1087	PERKIN-ELMER CORPORATION	54	
3	1087	SOLID STATE MATERIALS BRANCH	54	
4	1087	NORWALK, CONN. 06852	54	
1	1088	DR. R. C. OHLMANN	54	*
2	1088	WESTINGHOUSE RESEARCH LABORATORIES	54	
3	1088	PITTSBURGH, PENNA. 15235	54	
1	1089	PROFESSOR S. CLAESSON	54	*
2	1089	UPPSALA UNIVERSITY	54	
3	1089	UPPSALA, SWEDEN	54	
1	1106	COMMANDING OFFICER	54	
2	1106	OFFICE OF NAVAL RESEARCH BRANCH OFFICE	54	
3	1106	BOX 39, FPO	54	
4	1106	NEW YORK, NEW YORK 09510	54	
1	1122	DR. C. B. ELLIS	54	*
2	1122	GPL DIVISION	54	
3	1122	GENERAL PRECISION, INC.	54	
4	1122	63 BEDFORD ROAD	54	
5	1122	PLEASANTVILLE, NEW YORK 10570	54	
1	1172	MR. C. M. STICKLEY	54	
2	1172	AIR FORCE CAMBRIDGE RESEARCH	54	
3	1172	LABORATORIES - CROL	54	
4	1172	LAURENCE G. HANSCOM FIELD	54	
5	1172	BEDFORD, MASSACHUSETTS 01731	54	
1	1179	DR. RAY HOSKINS	54	*
2	1179	KORAD CORPORATION	54	
3	1179	2520 COLORADO AVENUE	54	
4	1179	SANTA MONICO, CALIFORNIA 90406	54	

1	1180	J. W. CARSON	54	*
2	1180	HUGHES AIRCRAFT COMPANY	54	
3	1180	CULVER CITY, CALIFORNIA 90230	54	
1	1183	PROF. A. SMAKULA	54	
2	1183	CRYSTAL PHYSICS LAB	54	
3	1183	MASSACHUSETTS INSTITUTE OF TECHNOLOGY	54	
4	1183	CAMBRIDGE, MASS 02139	54	
1	1184	DR. F. MCCLUNG	54	*
2	1184	HUGHES RESEARCH LABORATORIES	54	
3	1184	3011 MALIBU CANYON ROAD	54	
4	1184	MALIBU, CALIFORNIA 90265	54	
1	1186	PROF. G. W. STROKE	54	*
2	1186	ELECT. ENGINEERING DEPT.	54	
3	1186	THE UNIVERSITY OF MICHIGAN	54	
4	1186	ANN ARBOR, MICHIGAN 48107	54	
1	1212	AIR FORCE WEAPONS LABORATORY	54	
2	1212	KIRTLAND AIR FORCE BASE, NEW MEXICO 87118	54	
3	1212	ATTN APPLICATIONS DIVISION,	54	
4	1212	CAPTAIN P. JACKSON	54	
1	1213	BATTELLE MEMORIAL INSTITUTE	54	
2	1213	DEFENDER DOCUMENT LIBRARY	54	
3	1213	505 KING AVENUE	54	
4	1213	COLUMBUS, OHIO 43201	54	
5	1213	ATTN MR. JAMES OTT	54	
1	1214	AIR FORCE WEAPONS LABORATORY	54	
2	1214	KIRTLAND AIR FORCE BASE, NEW MEXICO 87118	54	
3	1214	ATTN LASER GROUP, MAJOR T. DOSS	54	
1	1215	AIR FORCE WEAPONS LABORATORY	54	
2	1215	KIRTLAND AIR FORCE BASE, NEW MEXICO 87118	54	
3	1215	ATTN CAPT. D. A. HAYCOCK, USAF	54	
1	1216	INSTITUTE FOR DEFENSE ANALYSES	54	
2	1216	400 ARMY-NAVY DRIVE	54	
3	1216	ARLINGTON, VIRGINIA 22202	54	
4	1216	ATTN DR. W. CULVER	54	
1	1232	UNIVERSITY OF TORONTO	54	*
2	1232	DEPARTMENT OF PHYSICS	54	
3	1232	TORONTO, ONTARIO, CANADA	54	
4	1232	ATTN B. STOICHEFF	54	
1	1233	ELECTRO-OPTICAL SYSTEMS, INC.	54	*
2	1233	300 N. HALSTEAD STREET	54	
3	1233	PASADENA, CALIFORNIA 91107	54	
4	1233	ATTN G. L. CLARK	54	
1	1234	SYRACUSE UNIVERSITY	54	
2	1234	SYRACUSE, NEW YORK 13210	54	
3	1234	ATTN G. K. WESSEL	54	

1	1235	THE PENNSYLVANIA STATE UNIVERSITY	54	
2	1235	101 OSMOND LABORATORY	54	
3	1235	UNIVERSITY PARK, PENNSYLVANIA 16802	54	
4	1235	ATTN D. H. RANK	54	
1	1236	MASSACHUSETTS INSTITUTE OF TECHNOLOGY	54	*
2	1236	DIVISION OF SPONSORED RESEARCH	54	
3	1236	CAMBRIDGE, MASSACHUSETTS 02139	54	
4	1236	ATTN J. DUCUING	54	
1	1237	BAUSCH AND LOMB, INC.	54	*
2	1237	ROCHESTER, NEW YORK 14602	54	
3	1237	ATTN A. F. TURNER	54	
1	1238	GENERAL ELECTRIC COMPANY	54	*
2	1238	ADVANCED PLANNING LABORATORIES	54	
3	1238	SCHENECTADY, NEW YORK 12301	54	
4	1238	ATTN K. F. TITTLE	54	
1	1239	SAN FERNANDO VALLEY STATE COLLEGE	54	*
2	1239	18111 NORDHOFF STREET	54	
3	1239	NORTHRIDGE, CALIFORNIA 91324	54	
4	1239	ATTN STEPHEN S. FRIEDLAND	54	
1	1240	D. B. ANDERSON	54	*
2	1240	AUTONETICS	54	
3	1240	3370 EAST ANAHEIM ROAD	54	
4	1240	ANAHEIM, CALIF. 92803	54	
1	1241	UNIVERSITY OF CALIFORNIA	54	*
2	1241	LOS ANGELES, CALIFORNIA 90024	54	
3	1241	ATTN M. A. EL-SAYED	54	
1	1242	TRW SYSTEMS, INC	54	*
2	1242	ONE SPACE PARK	54	
3	1242	REDONDO BEACH, CALIFORNIA 90278	54	
4	1242	ATTN S. ALTSHULER	54	
1	1243	UNIVERSITY OF CALIFORNIA	54	*
2	1243	DEPARTMENT OF PHYSICS	54	
3	1243	BERKELEY, CALIFORNIA 94720	54	
4	1243	ATTN Y. R. SHEN	54	
1	1244	P. A. FRANKEN	54	*
2	1244	LEAR SIEGLER, INC	54	
3	1244	2320 WASHTENAW AVENUE	54	
4	1244	ANN ARBOR, MICHIGAN 48104	54	
1	1246	DR. H. H. CASPERS	54	*
2	1246	NAVAL ORDNANCE LABORATORY	54	
3	1246	CORONA, CALIFORNIA 91720	54	
1	1250	Mr. B. G. Benak	54	*
2	1250	Union Carbide Corp., Electronics Div.	54	
3	1250	427 Chestnut Street, P. O. Box 985	54	
4	1250	Union, New Jersey 07083	54	

1	0225	DIRECTOR OF RESEARCH & DEVELOPMENT		54
2	0225	ARMY ORDNANCE MISSILE COMMAND		54
3	0225	HUNTSVILLE, ALABAMA 35801		54
4	0225	ATTN MR. WILLIAM D. MCKNIGHT		54
1	0226	OFFICE, CHIEF OF NAVAL OPERATIONS /OP-07T-1/		54
2	0226	DEPARTMENT OF THE NAVY		54
3	0226	WASHINGTON, D. C. 20301		54
4	0226	ATTN MR. BEN ROSENBERG		54
1	0227	BUREAU OF NAVAL WEAPONS /RR-2/		54
2	0227	DEPARTMENT OF THE NAVY		54
3	0227	WASHINGTON, D. C. 20360		54
4	0227	ATTN DR. C. H. HARRY		54
1	0228	BUREAU OF SHIPS /CODE 305/		54
2	0228	DEPARTMENT OF THE NAVY		54
3	0228	WASHINGTON, D. C. 20360		54
4	0228	ATTN DR. JOHN HUTH		54
1	0229	OFFICE OF NAVAL RESEARCH /CODE 402C/		54
2	0229	DEPARTMENT OF THE NAVY		54
3	0229	WASHINGTON, D. C. 20360		54
4	0229	ATTN DR. SIDNEY REED		54
1	0230	OFFICE OF NAVAL RESEARCH /CODE 421/	3 COPIES	54
2	0230	DEPARTMENT OF THE NAVY		54
3	0230	WASHINGTON, D. C. 20360		54
4	0230	ATTN MR. FRANK B. ISAKSON		54
1	0231	OFFICE OF NAVAL RESEARCH /CODE 406T/		54
2	0231	DEPARTMENT OF THE NAVY		54
3	0231	WASHINGTON, D. C. 20360		54
4	0231	ATTN MR. J. W. SMITH		54
1	0232	NAVAL RESEARCH LABORATORY /CODE 6440/		54
2	0232	DEPARTMENT OF THE NAVY		54
3	0232	WASHINGTON, D. C. 20390		54
4	0232	ATTN DR. C. C. KLICK		54
1	0233	NAVAL RESEARCH LABORATORY /CODE 7360/		54
2	0233	DEPARTMENT OF THE NAVY		54
3	0233	WASHINGTON, D. C. 20390		54
4	0233	ATTN DR. L. F. DRUMMETER		54
1	0234	HEADQUARTERS USAF /AFRDR-NU-3/		54
2	0234	DEPARTMENT OF THE AIR FORCE		54
3	0234	WASHINGTON, D. C. 20004		54
4	0234	ATTN LTCOL TERREL		54
1	0235	RESEARCH & TECHNOLOGY DIVISION		54
2	0235	BOLLING AFB		54
3	0235	WASHINGTON, D. C. 20332		54
4	0235	ATTN MR. ROBERT FEIK		54

1	1267	DR. J. C. ALMASI	54	*
2	1267	GENERAL ELECTRIC	54	
3	1267	ADVANCED RESEARCH LABORATORY	54	
4	1267	SCHENECTADY, N. Y. 12305	54	
1	1268	DR. P. J. WAGNER	54	*
2	1268	DEPARTMENT OF CHEMISTRY	54	
3	1268	MICHIGAN STATE UNIVERSITY	54	
4	1268	EAST LANSING, MICH. 48823	54	
1	1269	DR. A. J. DEMARIA	54	*
2	1269	RESEARCH LABORATORY	54	
3	1269	UNITED AIRCRAFT CORPORATION	54	
4	1269	EAST HARTFORD CONN 06108	54	
1	1270	DR. C. H. CHURCH	54	*
2	1270	WESTINGHOUSE ELECTRIC CORPORATION	54	
3	1270	RESEARCH AND DEVELOPMENT CENTER	54	
4	1270	PITTSBURGH, PA. 15235	54	

FURTHER ADDITIONS TO LIST 54

Robert L. Parker
National Bureau of Standards
Washington, D. C.

Authorized by letter
ONR:421:CES:lm
NR 017-708 - 30 November 1964

N. D. Schoenberger
Precision Instrument Company
3170 Porter Drive
Palo Alto, California

ONR:421:FBI:lsp
13 Nov. 1964

University of California
Lawrence Radiation Laboratory
Attn: Technical Information Division
P. O. Box 808
Livermore, California 94551

Authorized by Distribution List
Change Request NAVEXOS 3703 (4-60)

ONR:421:F. B. Isakson
NR 017-710
2 August 1965

Radio Corporation of America
David Sarnoff Research Center
Attn: Dr. R. J. Pressley
Princeton, New Jersey

Authorized by Distribution List
Change Request NAVEXOS 3703 (4-60)

ONR:421:F. B. Isakson
NR 017-710
2 August 1965

Nonr 4132(00)
U. S. Army Electronics Command
Attn: AMSEL-PP-IED-2B
Mr. J. E. Sanders
225 S. 18th Street
Philadelphia, Pennsylvania 19103

Authorized by Distribution List
Change Request NAVEXOS 3703 (4-60)

ONR:421:F. B. Isakson
NR 017-710
24 February 1966

Commanding Officer
Frankford Arsenal
Philadelphia, Pennsylvania 19137
Attn: J. H. Fiergus
Building 110-2

Authorized by Distribution List
Change Request NAVEXOS 3703 (4-60)
ONR:421:F. B. Isakson
NR No. 017-710
2 February 1966

U. S. Naval Research Laboratory
Attn: Dr. W. H. Vaughan, Code 6430
Washington, D. C. 20390

Authorized by Distribution List
Change Request NAVEXOS 3703 (4-60)
ONR:421:F. B. Isakson
NR No. 017-710
23 March 1966

FURTHER ADDITIONS TO LIST 54 (continued)

Mr. S. A. Ramsden
Division of Pure Physics
National Research Council
Ottawa 2, Canada

Authorized by Distribution List
Change Request NAVEXOS 3703 (4-60)
ONR:421:F. B. Isakson
NR No. 017-710
30 September 1966

Stanford Research Institute
Attn: G-037, External Reports
for: Walter Nelson
Menlo Park, California 94025

Authorized by Distribution List
Change Request NAVEXOS 3703 (4-60)
ONR:421:F. B. Isakson
NR No. 017-710
25 October 1966

UNCLASSIFIED

Security Classification

DOCUMENT CONTROL DATA - R&D

(Security classification of title, body of abstract and indexing annotation must be entered when the overall report is classified)

1. ORIGINATING ACTIVITY *(Corporate author)*
Union Carbide Corporation, Electronics Division
Crystal Products R and D
Indianapolis, Indiana

2a. REPORT SECURITY CLASSIFICATION
Unclassified

2b GROUP

3. REPORT TITLE
Czochralski Ruby, Annual Technical Summary Report

4. DESCRIPTIVE NOTES *(Type of report and inclusive dates)*
Annual Technical Summary Report: January 1, 1966 - December 31, 1966

5. AUTHOR(S) *(Last name, first name, initial)*
Keig, George A.
Nestor, O. H.
Otten, Peter E.

6. REPORT DATE	7a. TOTAL NO. OF PAGES	7b. NO. OF REFS
March 20, 1967	37	14

8a. CONTRACT OR GRANT NO.	9a. ORIGINATOR'S REPORT NUMBER(S)
Nonr-4132(00)	SRCR-67-5
b. PROJECT NO.	
c.	9b. OTHER REPORT NO(S) *(Any other numbers that may be assigned this report)*
d.	

10. AVAILABILITY/LIMITATION NOTICES

11. SUPPLEMENTARY NOTES	12. SPONSORING MILITARY ACTIVITY
	Office of Naval Research Department of the Navy Washington, D. C. 20360

13. ABSTRACT

The Czochralski growth technique has been developed to yield large ruby crystals with optical quality suitable for use as solid state lasers. This has involved a scale-up of the present growth process to produce crystals 2 inches in diameter and 12 inches long. The material properties of the ruby have been studied with special attention given to its behavior during active lasing. The properties receiving attention have been chromium distribution and the identification and removal of inclusions causing laser damage during Q-switched operation.

DD FORM 1 JAN 64 1473

UNCLASSIFIED

Security Classification

14. KEY WORDS	LINK A		LINK B		LINK C	
	ROLE	WT	ROLE	WT	ROLE	WT
Czochralski growth Laser crystals Ruby Laser crystal damage						

INSTRUCTIONS

1. ORIGINATING ACTIVITY: Enter the name and address of the contractor, subcontractor, grantee, Department of Defense activity or other organization *(corporate author)* issuing the report.

2a. REPORT SECURITY CLASSIFICATION: Enter the overall security classification of the report. Indicate whether "Restricted Data" is included. Marking is to be in accordance with appropriate security regulations.

2b. GROUP: Automatic downgrading is specified in DoD Directive 5200.10 and Armed Forces Industrial Manual. Enter the group number. Also, when applicable, show that optional markings have been used for Group 3 and Group 4 as authorized.

3. REPORT TITLE: Enter the complete report title in all capital letters. Titles in all cases should be unclassified. If a meaningful title cannot be selected without classification, show title classification in all capitals in parenthesis immediately following the title.

4. DESCRIPTIVE NOTES: If appropriate, enter the type of report, e.g., interim, progress, summary, annual, or final. Give the inclusive dates when a specific reporting period is covered.

5. AUTHOR(S): Enter the name(s) of author(s) as shown on or in the report. Enter last name, first name, middle initial. If military, show rank and branch of service. The name of the principal author is an absolute minimum requirement.

6. REPORT DATE: Enter the date of the report as day, month, year, or month, year. If more than one date appears on the report, use date of publication.

7a. TOTAL NUMBER OF PAGES: The total page count should follow normal pagination procedures, i.e., enter the number of pages containing information.

7b. NUMBER OF REFERENCES: Enter the total number of references cited in the report.

8a. CONTRACT OR GRANT NUMBER: If appropriate, enter the applicable number of the contract or grant under which the report was written.

8b, 8c, & 8d. PROJECT NUMBER: Enter the appropriate military department identification, such as project number, subproject number, system numbers, task number, etc.

9a. ORIGINATOR'S REPORT NUMBER(S): Enter the official report number by which the document will be identified and controlled by the originating activity. This number must be unique to this report.

9b. OTHER REPORT NUMBER(S): If the report has been assigned any other report numbers *(either by the originator or by the sponsor)*, also enter this number(s).

10. AVAILABILITY/LIMITATION NOTICES: Enter any limitations on further dissemination of the report, other than those imposed by security classification, using standard statements such as:

(1) "Qualified requesters may obtain copies of this report from DDC."

(2) "Foreign announcement and dissemination of this report by DDC is not authorized."

(3) "U. S. Government agencies may obtain copies of this report directly from DDC. Other qualified DDC users shall request through _____."

(4) "U. S. military agencies may obtain copies of this report directly from DDC. Other qualified users shall request through _____."

(5) "All distribution of this report is controlled. Qualified DDC users shall request through _____."

If the report has been furnished to the Office of Technical Services, Department of Commerce, for sale to the public, indicate this fact and enter the price, if known.

11. SUPPLEMENTARY NOTES: Use for additional explanatory notes.

12. SPONSORING MILITARY ACTIVITY: Enter the name of the departmental project office or laboratory sponsoring *(paying for)* the research and development. Include address.

13. ABSTRACT: Enter an abstract giving a brief and factual summary of the document indicative of the report, even though it may also appear elsewhere in the body of the technical report. If additional space is required, a continuation sheet shall be attached.

It is highly desirable that the abstract of classified reports be unclassified. Each paragraph of the abstract shall end with an indication of the military security classification of the information in the paragraph, represented as *(TS)*, *(S)*, *(C)*, or *(U)*.

There is no limitation on the length of the abstract. However, the suggested length is from 150 to 225 words.

14. KEY WORDS: Key words are technically meaningful terms or short phrases that characterize a report and may be used as index entries for cataloging the report. Key words must be selected so that no security classification is required. Identifiers, such as equipment model designation, trade name, military project code name, geographic location, may be used as key words but will be followed by an indication of technical context. The assignment of links, rules, and weights is optional.